

# Effect of Heat Treatment on the Efficiency of Mg Anodes

B. Campillo, C. Rodriguez, J. Genesca, J. Juarez-Islands, O. Flores, and L. Martinez

Commercial magnesium anodes were evaluated using ASTM G 97-89 for a standard test along with a technique of electrochemical impedance. Several heat treatments were performed, and the anodic efficiency was determined, showing an incremental increase of 10 to 12 % of the efficiency demonstrated by the nontreated commercial anodes (as-cast condition). The increase in efficiency was related to the microstructural characteristics. The appearance of second phase particles influenced the form of the corrosion process.

**Keywords** cathodic protection, magnesium, magnesium heat treatment

## 1. Introduction

The increasing demand for cathodic protection in the past few years for commercial and domestic uses gave rise to widespread interest in new developments and applications of galvanic anodes. A considerable amount of work was completed to improve the most important properties of the anodes considering mainly the metal purity (Ref 1), the alloying elements (Ref 2, 3), and backfill material (Ref 4). These studies concentrated efforts toward improvements in current efficiency, polarization characteristics, and the distribution of the corrosion attack in the anodes.

Magnesium anodes are particularly recommended for high-resistivity environments where inherent negative potential and high current output per unit weight is desirable (capacity to drain the current [Ref 5]). Magnesium anodes generally have a current efficiency lower than that of other galvanic anodes. In practice, current efficiency rarely exceeds 50%. This figure is unfavorable compared to that of other anodes, such as zinc and aluminum that have current efficiencies that exceed 90%. Several factors were attributed to the low efficiency of the magnesium anodes, such as the thermal history related to the structure effects and the alloying elements (Ref 3, 4, 6), changes in anion and cation concentrations that occur close to the dissolving magnesium surface, and the anodic electrochemistry (Ref 7).

Consumers of magnesium-base sacrificial anodes are concerned with the casting procedures and the efficiency of the sacrificial anode material that ranges between 30 and 35%. Cathodic protection is well established and required by law for pipeline protection. There is, therefore, current interest in improving the efficiency of magnesium anodes. Salinas and Besone (Ref 8) pointed out that the metallurgical features of sacrificial anodes (casting conditions, heat treatments, etc.) are related to the anode operation potential and to their own efficiency. In the magnesium anodes, contrary to the requirements for anode materials, the corrosion occurs by pitting rather than by uniform corrosion, thus shifting the potential to more elec-

tronegative values (Ref 9). However, recent work (Ref 10) reported that pitting was found under a local (Ref 11) standard that used artificial sea water for the anode evaluation. Furthermore, Lee et al. (Ref 10) report that when using the ASTM standard for GALVOMAG (Dow Chemical Co.) type anode evaluation, uniform corrosion was found. This difference was due to the solution used.

Conversely, local consumers of magnesium anodes pointed out that they have several tons of low-efficiency magnesium anodes already cast in stock, and they are interested in rehabilitating these anodes rather than rejecting them. The low-efficiency is related to the heterogeneity of their chemical composition obtained from several batches of anodes (i.e., higher ratios iron/magnesium as specified by ASTM). Recent work (Ref 12, 13) completed in the authors' laboratories concentrated on this situation, and the efficiency was reported to improve up to 60% by modifying the solidification processes and thus controlling the amount of second phase particles at grain boundaries. This produced a more uniform distribution of impurities in the matrix. The purpose of the present work is to seek an alternative to improve the anode efficiency by using heat treatments and/or different cooling rates to directly use the cast anodes instead of refining them and, where possible, to correlate the microstructural observations with the efficiency obtained.

## 2. Experimental Procedures

A commercial magnesium anode of bulk chemical composition (in wt%) 0.012% Cu, 0.056% Fe, 1.260% Mn, 0.007% Ni, and 0.004% Al and magnesium balance was used for this study. The chemical analysis was performed according to the ASTM standard. From the composition, it was clear that the iron value was high compared to the typical value of 0.03% reported for these types of anodes. Also, the nickel content is above the typical value of 0.001%. Several cuttings were performed according to ASTM G 97-89 (Ref 14) to obtain cylindrical anodes. The dimensions of the test anodes were 152 by 12.7 mm, and special care during machining was necessary to avoid heating. These anodes were lapped to a 240 grit finish, thoroughly cleaned, and weighed before the electrochemical evaluation was carried out to assess the effect of heat treatments on the commercial anode, using the same specimens obtained for the ASTM tests. Several cooling rates were used (50, 400, and 1000 °C/s) under an argon atmosphere using several holding times at each temperature. The heating temperature was 400 °C, and from this, the cooling rates were determined.

**B. Campillo, C. Rodriguez, and J. Genesca**, Facultad de Química, UNAM, Edif. D. CU, Mexico DF 04510; **J. Juarez-Islands**, Inst. de Inv. de Materiales-UNAM, CU, Mexico DF 04510; **O. Flores** and **L. Martinez**, Lab. Cuernavaca, IFUNAM, P.O. Box 48-3, C.P. 62251, Cuernavaca, Mor. Mexico.

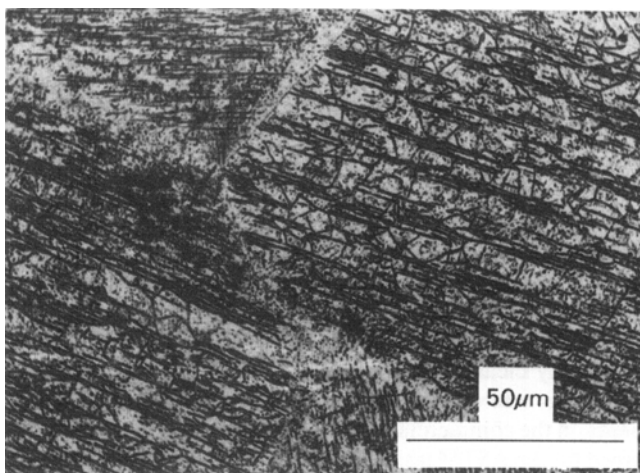
Also, two aging treatments were performed using 400 and 300 °C as the solution temperatures at different times ranging from 1.8 to 57.6 ks, followed by a water quench. The aging temperature was 250 and 150 °C, respectively, at different holding times (from 1.8 to 57.6 ks). Table 1 shows the thermal treatments completed in this work. Metallographic specimens were prepared and photomicrographs were taken with both an optical and a scanning electron microscope (SEM) equipped with an energy dispersive x-ray spectrometer. The sacrificial anodes with and without heat treatment were evaluated electrochemically according to ASTM G 97-89 with the standard laboratory test method for magnesium sacrificial anodes for underground applications (Ref 14). For this test, a known direct current is

passed through a test cell connected in series (galvanostatic method). Each test cell consists of a preweighed magnesium anode specimen, a steel pot container, and a solution of  $\text{CaSO}_4 + \text{Mg}(\text{OH})_2$ . The oxidation potential of the specimens is measured several times during the 14 day test and 1 h after the current is turned off. At the conclusion of the test, each specimen is cleaned and weighed. The ampere hours obtained per unit mass of specimen loss are calculated. The values obtained are shown in Table 2; these values represent an average from five test specimens. Also, the closed and open circuit potential average values are shown. After assessment of the current efficiency, the specimens were observed under SEM at 25 kV.

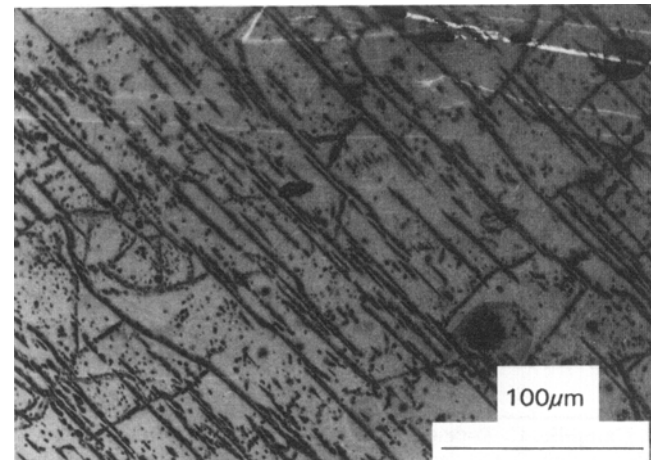
**Table 1** Electrochemical efficiency of the anodes after thermal treatments

Condition	Efficiency (a), %	Circuit potential (b), mV	
		Open	Closed
As-cast	45.73	-1686	-1558
Furnace cooled ( $\approx 50$ °C/s), 400 °C/18 ks (c)	30.42	-1499	-1478
Furnace cooled ( $\approx 50$ °C/s), 400 °C/28.8 ks	26.53	-1591	-1581
Furnace cooled ( $\approx 50$ °C/s), 400 °C/57.6 ks	25.78	-1600	-1572
Cooled in air ( $\approx 400$ °C/s), 400 °C/18 ks	42.03	-1714	-1497
Cooled in air ( $\approx 400$ °C/s), 400 °C/28.8 ks	10.42	-1584	-1568
Cooled in air ( $\approx 400$ °C/s), 400 °C/57.6 ks	8.99	-1620	-1595
Solution treated 400 °C/1.8 ks, water cooled ( $\approx 1000$ °C/s); aged 150 °C/1.8 ks	47.5	-1517	-1576
Solution treated 400 °C/18 ks, water cooled ( $\approx 1000$ °C/s); aged 250 °C/18 ks	23.5	-1713	-1585
Solution treated 400 °C/28.8 ks, water cooled ( $\approx 1000$ °C/s); aged 250 °C/28.8 ks	33.05	-1777	-1590
Solution treated 400 °C/57.6 ks, water cooled ( $\approx 1000$ °C/s); aged 250 °C/57.6 ks	22.98	-1789	-1550
Solution treated 300 °C/1.8 ks, water cooled ( $\approx 1000$ °C/s); aged 150 °C/1.8 ks	52.77	-1495	-1483
Solution treated 300 °C/18 ks, water cooled ( $\approx 1000$ °C/s); aged 150 °C/18 ks	60.77	-1614	-1503
Solution treated 300 °C/28.8 ks, water cooled ( $\approx 1000$ °C/s); aged 150 °C/28.8 ks	63.85	-1661	-1480
Solution treated 300 °C/57.6 ks, water cooled ( $\approx 1000$ °C/s); aged 150 °C/57.6 ks	56.43	-1492	-1482

(a) These values represent an average for 5 test specimens. (b) These represent average values of the circuit potential. (c) Kilosecond holding time



(a)



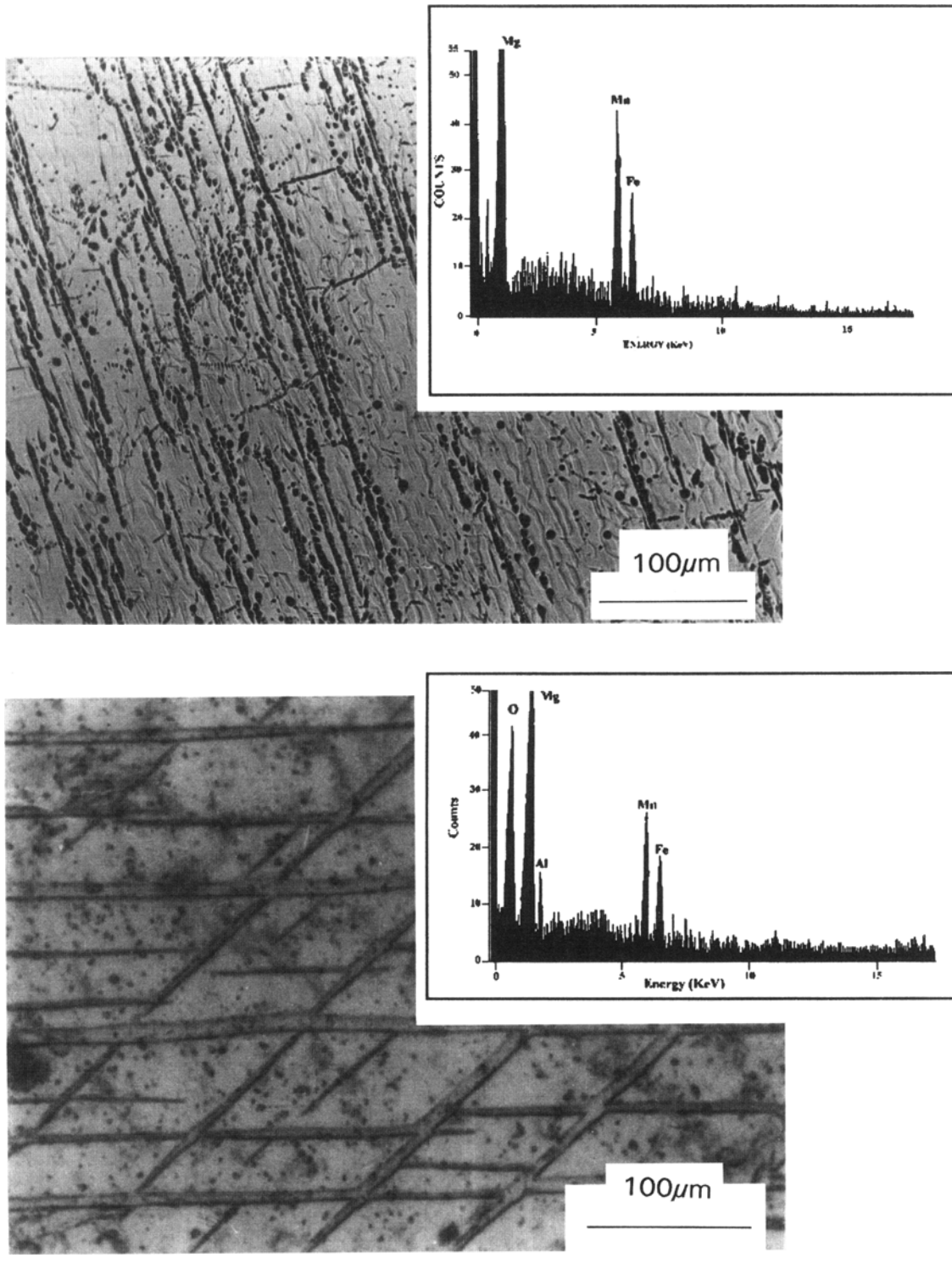
(b)

**Fig. 1** (a) Microstructure of the anode in the as-received condition. (b) Detail of the microstructure of the anode in the as-received condition

### 3. Results and Discussion

Figure 1 shows a micrograph of the microstructure of the anode in the as-received condition, the microstructure of columnar grains, and the inside of the columnar grains where a

substructure is formed by equiaxed grains. The size is approximately 100  $\mu\text{m}$  in the center of the anode (Fig. 1a). The microstructure consists mainly of columnar grains of  $\alpha\text{Mg}$ . Few precipitates were observed at the interior of the columnar grains at the equiaxed grains and at the grain boundaries



(b)

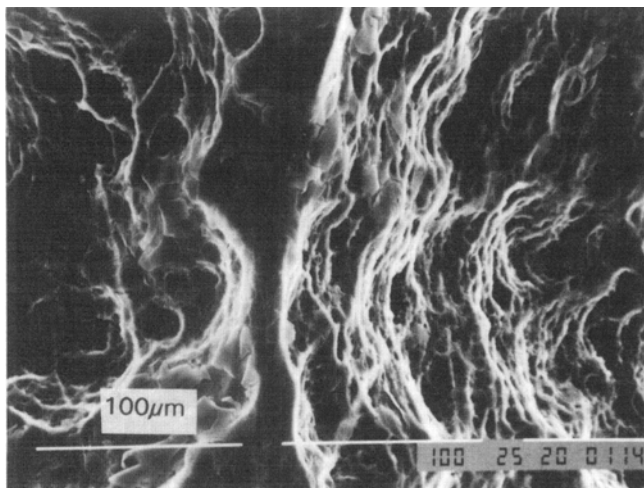
**Fig. 2** (a) Microstructure of the anode cooled in air (400 °C/28.8 ks) with the EDAX pattern. (b) Microstructure of the anode solution treated at 300 °C and aged 28.8 ks at 150 °C with the EDAX pattern

(Fig. 1b). The microanalysis detected that the precipitates observed were rich in iron and manganese similar to the inset electron dispersive analysis by x-ray (EDAX) pattern in Fig. 2(a). The heat treatments performed in the as-cast anodes substantially modified the microstructure and the microanalysis of the precipitates. Figure 2(a) shows a micrograph obtained when the as-cast anode was heat treated and cooled in air, demonstrating columnar type structure with a substructure inside the columnar grains with very fine precipitates. These precipitates were concentrated near the grain boundaries. Microana-

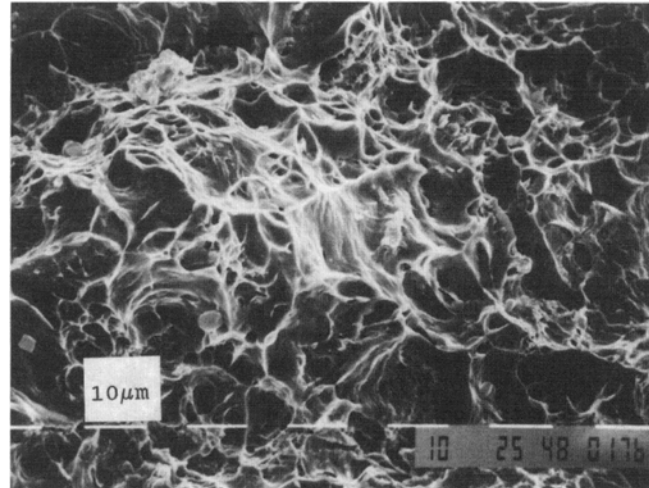
lysis indicates the presence of iron and manganese in these fine precipitates and a relatively high concentration of manganese being segregated as a second phase particle (diagram in the inset). Figure 2(b) is the microstructure obtained from the anode being solution treated at 300 °C and then aged during 28.8 ks at 150 °C. It shows a needlelike structure associated with very fine precipitates distributed in the matrix, and the microanalysis showed the presence of iron, manganese, magnesium, and aluminum (diagram in the inset). The formation of aluminum and magnesium particles at the grain boundaries indicates that

**Table 2 Microstructural parameters of the magnesium anodes after thermal treatments**

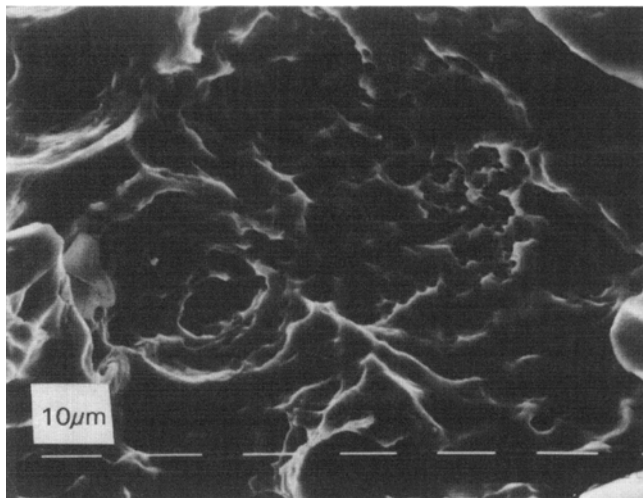
Condition	Columnar grain size range, $\mu\text{m}$	Particle size range, $\mu\text{m}$	Morphology	Elements detected by EDAX
As cast	100-160	10-12	Spherical-irregular	Fe-Mn (Fe rich)
Air cooled	120-180	8-9	Spherical-irregular	Fe-Mn
Furnace cooled	120-200	8-10	Spherical	Fe-Mn
Aged	180-250	1-3	Spherical	Mg-Al, Fe-Mn



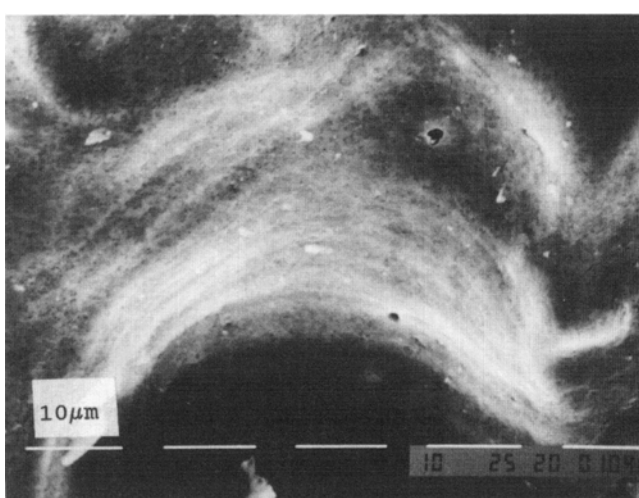
(a)



(b)



(c)



(d)

**Fig. 3** (a) SEM micrograph of the anode in the as-received condition after the ASTM test. (b) SEM micrograph of the anode aged (400 °C/18 ks) after the ASTM test. (c) SEM micrograph of the anode furnace cooled (400 °C/28.8 ks) after the ASTM test. (d) SEM micrograph of the anode aged (300 °C/28.8 ks) after the ASTM test

this treatment may have redissolved the iron-manganese particles to form manganese-rich second phase particles. Table 2 shows a history of the main microstructural parameters being observed and measured for the different heat treatments completed, and Table 1 shows the efficiency values obtained. From the data, it can be observed that the efficiency increases as the particle size tends to decrease, specifically for aging treatments at 300 °C. The morphology changes to spherical, and the chemistry of these particles changes with the appearance of the compound of aluminum-magnesium at the grain boundaries to help obtain a higher efficiency. This situation may be due to the presence of aluminum-magnesium compounds at the grain boundaries acting as local cathodes to the matrix. It was reported that the benefit of aluminum is related to the nature of an oxide of this type (magnesium-rich), which is thinner with increasing aluminum content (Ref 15). Also, there is a strong tendency for aluminum to form a stable passive film in a certain type of electrolyte, and there is lack of galvanic action between magnesium and aluminum in magnesium alloys.

The low efficiencies were related to the presence of insoluble particles of iron-manganese (iron-rich) that, together with the presence of manganese, segregated as a second phase. They were observed directly on samples cooled in air and/or furnaces. These precipitates and segregates are not uniformly distributed. In some places the manganese was segregated, and in other regions, only the iron-manganese particles were observed on the grain boundaries, indicating that during the corrosion test, the particles act as local galvanic microcells of strong cathodic nature.

After the ASTM tests, almost all anodes showed a nonuniform corrosion appearance when viewed with the naked eye or under low magnification. The surface of these specimens was observed more closely. Figure 3(a) is a scanning electron microscope (SEM) photomicrograph showing the anode in the as-cast condition after the ASTM test. It was observed that corrosion of magnesium occurs preferentially in regions rich in second phase, often subject to localized segregation, elemental depletion, or precipitation. Corrosion in these regions is by pitting and forms a steplike pattern. The pits were quite deep and, in many cases, showed cracks at their base. Figure 3(b) shows the surface appearance of an anode heat treated (aged 400 °C, during 18 ks) with a very low efficiency (23.5%). It can be observed that the corrosion pattern is almost similar to the pattern showed for the anode as-cast (Fig. 1a), that is, pitting and forming a steplike pattern. Figure 3(c) is an anode heat treated (furnace cooled, 400 °C/28.8 ks) and shows a pitted region. Such pits are very deep and certainly indicate accelerated nonuniform corrosive attack at high energy locations (grain boundaries and/or precipitates). Figure 3(d) shows uniform corrosion attack founded in the anodes heat treated (aged 300 °C, during 28.8 ks) with high efficiencies (60% or more). This pattern was obtained inside the pits uniformly distributed along the anode. This uniform attack was observed in almost all the anodes heat treated with high efficiencies. A few spherical particles were found and were roughly 1 μm in diameter. Such particles were rich in iron-manganese and widely distributed over the surface, inducing a relatively uniform attack.

From the results obtained in this work and considering recent reports (Ref 12, 13), values higher than 50% of efficiency were obtained, and these values are directly related to the mi-

crostructure/cooling rate (Table 1, 2) of the magnesium-anodes. For example, with the particle and/or grain size measured in the as-cast anodes, the cooling rate varied from 10<sup>3</sup> K/s (roughly 5 μm in particle size) to 10<sup>2</sup> K/s (roughly 10 μm in particle size), meaning a considerable refinement of the microstructure compared with the as-cast anodes that had particle and/or grain size of about 100 μm or larger. Conversely, impurities such as copper and nickel and second-phase particles rich in iron and aluminum were partially dissolved by the heat treatment (aged). This caused an increase in efficiency and overall uniform corrosion rather than localized corrosion (pitting).

## 4. Conclusions

- Using specific heat treatments, the efficiency of the magnesium anodes were improved. With this, it is possible to control the amount and size of the precipitates and the second-phase particles localized at grain boundaries and inside the matrix.
- Lower efficiency was related to the presence of manganese-rich second-phase particles where corrosion occurred along a narrow region at the grain boundaries.
- To ensure high efficiency of magnesium anodes, it is necessary to control the impurities that are uniformly distributed in solid solution and the microstructural parameters. The solution could be the use of an alternative casting process (Ref 12) and heat treatments.

## Acknowledgments

The authors are grateful for the technical support of L.A. Nuñez, J.L. Albarran, and A. Gonzalez. This work was supported by DGAPA-UNAM grant No. 1N101995 and the Facultad de Química-UNAM, Mexico.

## References

1. H.A. Robinson and P.F. George, *Corrosion*, Vol 10 (No. 6), 1954, p 182
2. H.A. Robinson, *Trans. J. Electrochem. Soc.*, Vol 90, 1946, p 485
3. J.D. Hanawalt, C.E. Nelson, and J.A. Peloubet, *Corrosion Studies of Mg and Its Alloys*, *Met. Technol.*, 1941
4. O. Osborn and H.A. Robinson, *Corrosion*, Vol 8 (No. 4), 1982, p 114
5. J.O.M. Bockris, N. Bociocat, and F. Gutmann, *An Introduction to Electrochemical Science*, Wykehampub, London, 1974
6. H. Jones, *J. Mater. Sci.*, Vol 19, 1984, p 1084
7. C.F. Schriber, *Sacrificial Anodes, Cathodic Protection—Theory and Practice*, Pergamon Press, Coventry, U.K., 1982
8. D.R. Salinas and J.B. Bessone, *Corrosion*, Vol 47 (No. 9), 1991, p 665
9. J.B. Bessone, R.A. Suarez, and S.M. De Micheli, *Corrosion*, Vol 37, 1981, p 533
10. J.C. Lee, C. Rodriguez, and J. Genesca, *Revista Afinidad*, Madrid, Spain
11. DGN Mexican Standard Norm for Mg-Anodes
12. J.A. Juarez-Islands, J. Genesca, and R. Perez, *JOM*, Sept 1985, p 42
13. J.A. Juarez-Islands, L. Martinez, and J. Genesca, *Corrosion 93*, Paper 536, NACE, 1993
14. ASTM Designation G 97-89, ASTM, 1989, p 1-4
15. A. Joshi and R. Lewis, in *Advances in Mg Alloys and Composites*, H. Paris and W.H. Hunt, Ed., The Met. Soc. AIME, 1989, p 89